Science Advances
AAAS

# Supplementary Materials for

## Genetic architecture of the white matter connectome of the human brain

Zhiqiang Sha *et al.*

Corresponding author: Clyde Francks, clyde.francks@mpi.nl

*Sci. Adv.* **9**, eadd2870 (2023)
DOI: 10.1126/sciadv.add2870

**The PDF file includes:**

Figs. S1 to S14
Legends for tables S1 to S31

**Other Supplementary Material for this manuscript includes the following:**

Tables S1 to S31

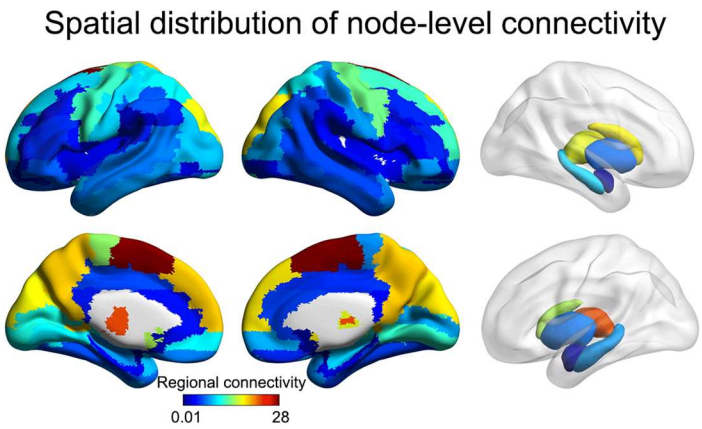


**Supplementary Figure 1. Spatial distribution of node-level connectivity.** The connectivity of each region of the AAL brain atlas was calculated as the sum of its white matter connections to all other regions (see Methods). Regions in orange-red colours had the highest connectivity.

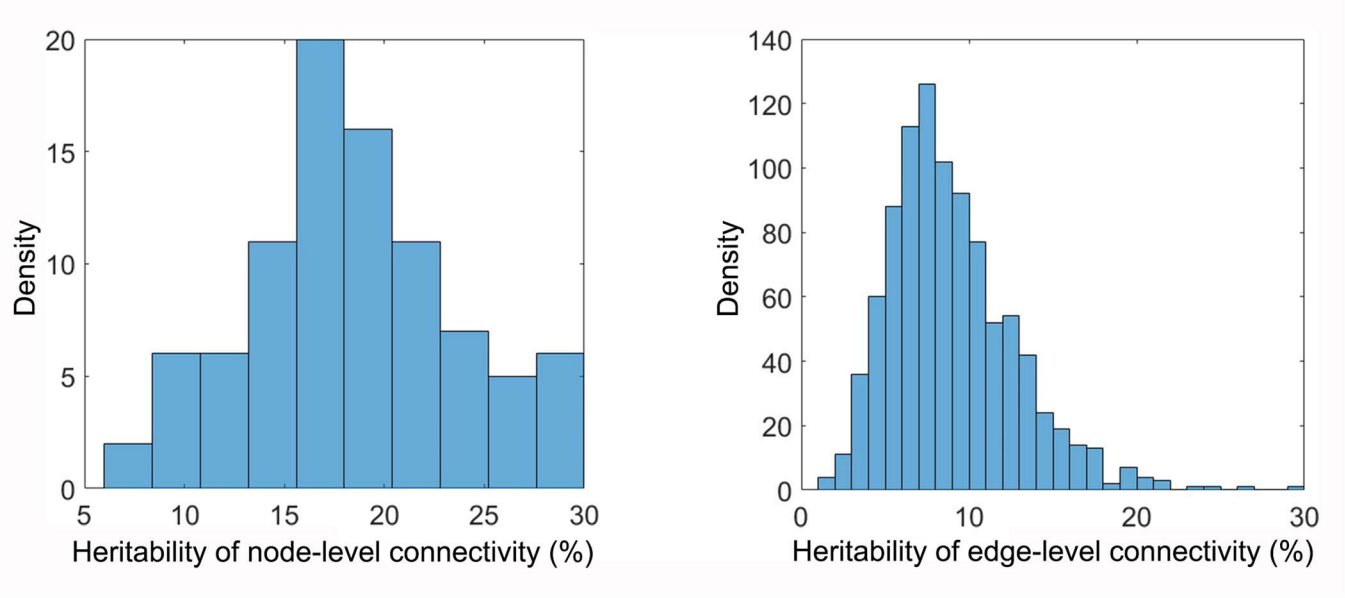


**Supplementary Figure 2. Frequency histograms showing the distributions of SNP-based heritabilities, separately for 90 node-level connectivities (Left panel) and 947 edge-level connectivities (Right panel).**

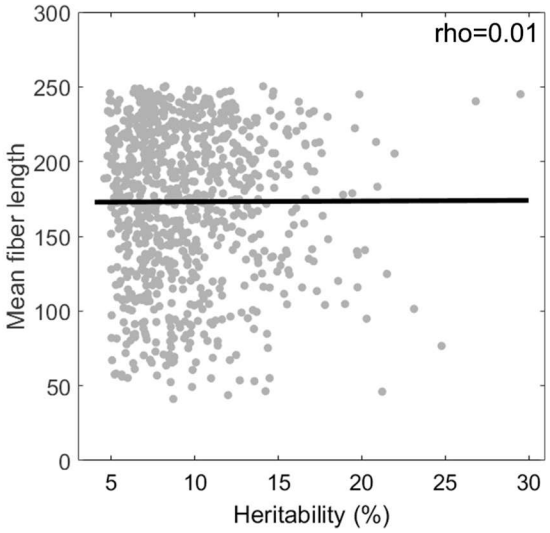


**Supplementary Figure 3. No significant correlation between SNP-based heritabilities and fiber lengths of edge-level connectivities.** Each dot represents an edge linking two brain regions defined in the AAL atlas.

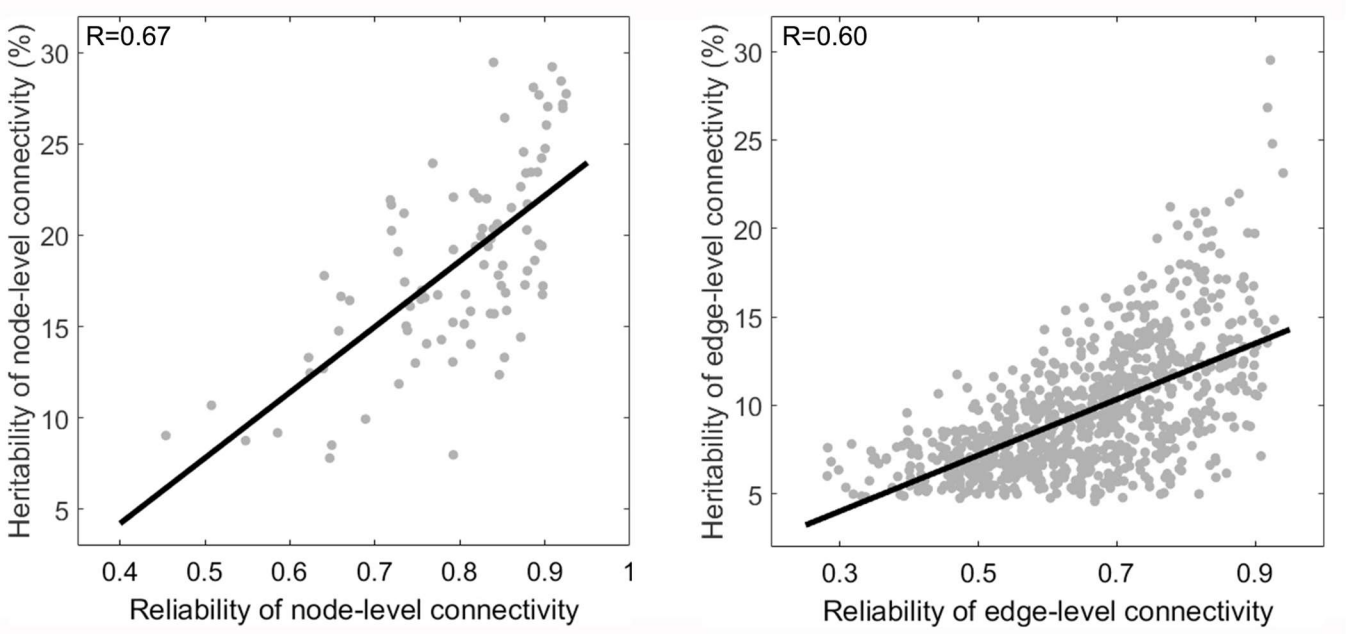


**Supplementary Figure 4. Correlations between reliability (intra-class correlation) and heritability, separately for 90 node-level connectivities (left) and 947 edge-level connectivities (right).**

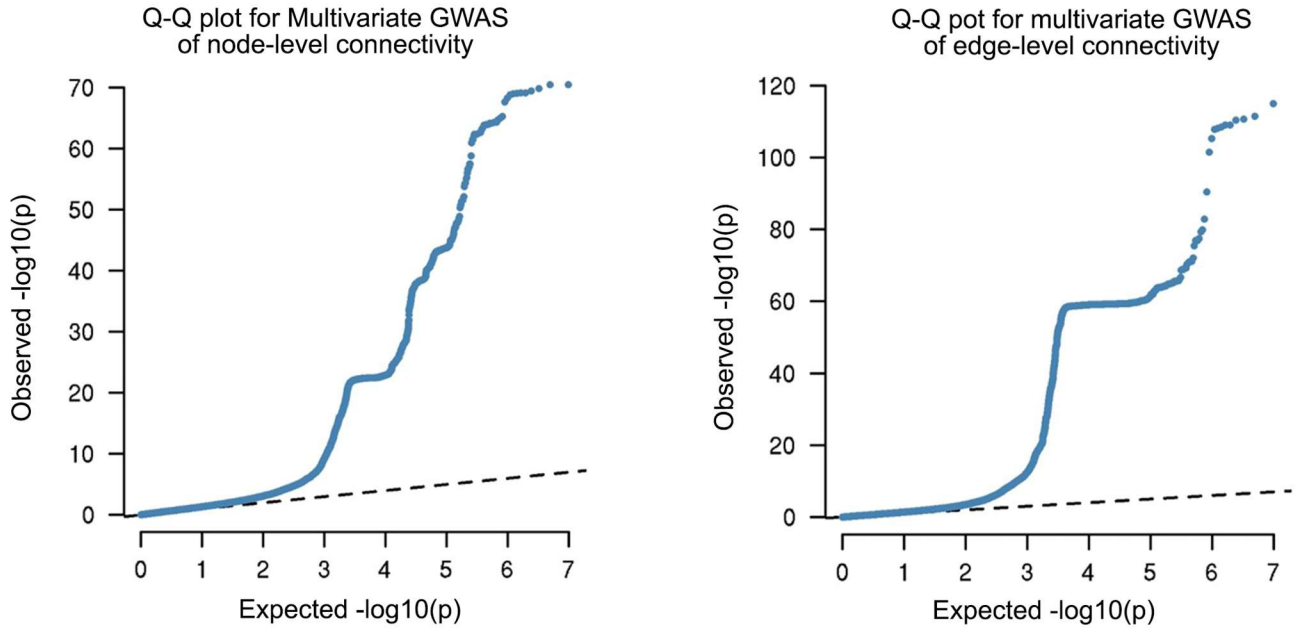


**Supplementary Figure 5. Q-Q plots of multivariate GWAS for node-level connectivity and edge-level connectivity**

Left panel: Q-Q plot of multivariate GWAS for node-level connectivity. Right panel: Q-Q plot of multivariate GWAS for edge-level connectivity. The black dotted line presents the observed –log10(p-values) from the multivariate GWAS plotted against the expected –log10(p-values) from a null distribution.

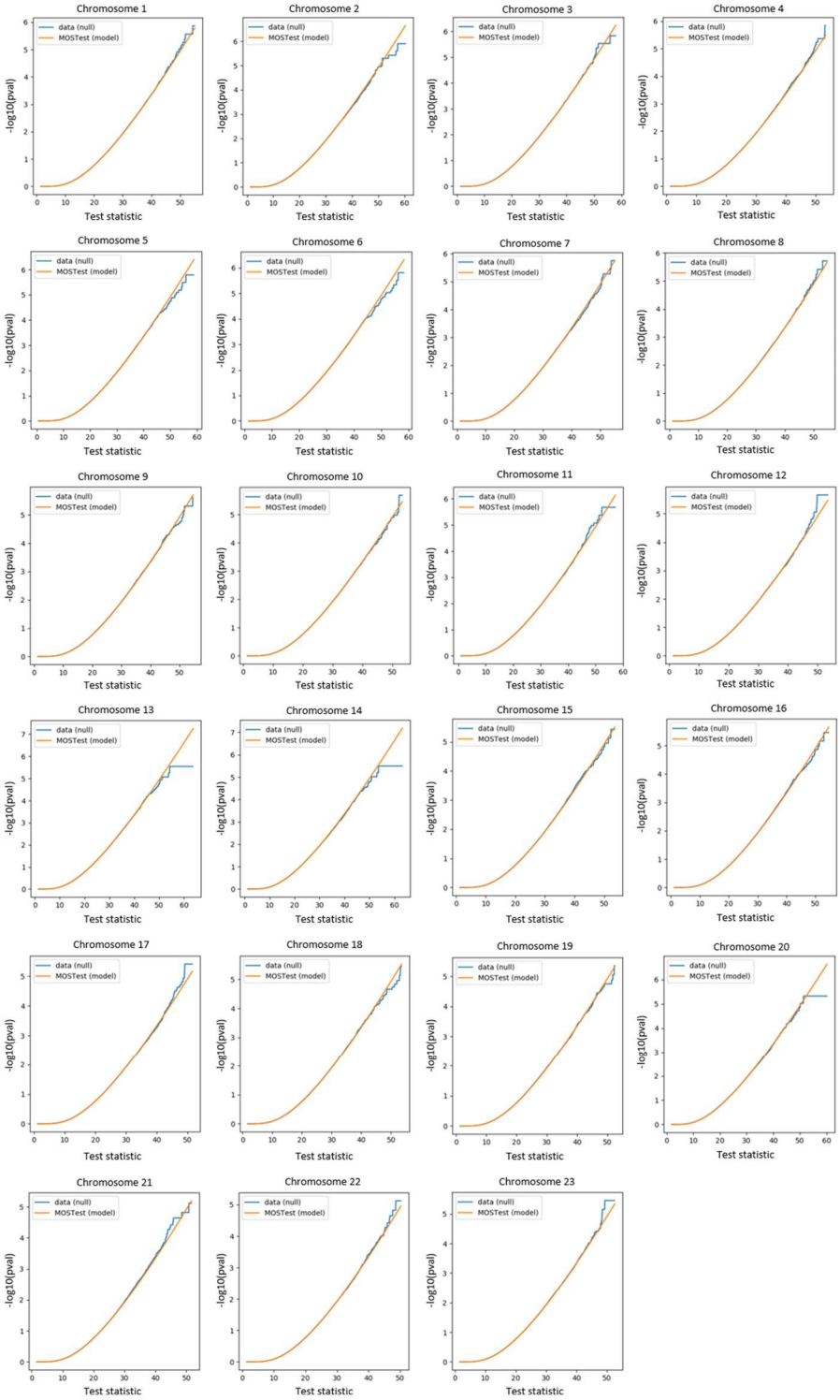


**Supplementary Figure 6. Permuted and analytic P value distributions under the null, for the multivariate GWAS of node-level connectivity.** Only null distributions are shown here, i.e. not the true association results. Close matching of the null p-value distributions from the permuted data (blue) and analytic forms (orange) indicate correct control of type 1 error. The analytic distribution can then be extrapolated to assess the significance of multivariate associations with far lower p values (see Methods). 'Chromosome 23' refers to chromosome X.

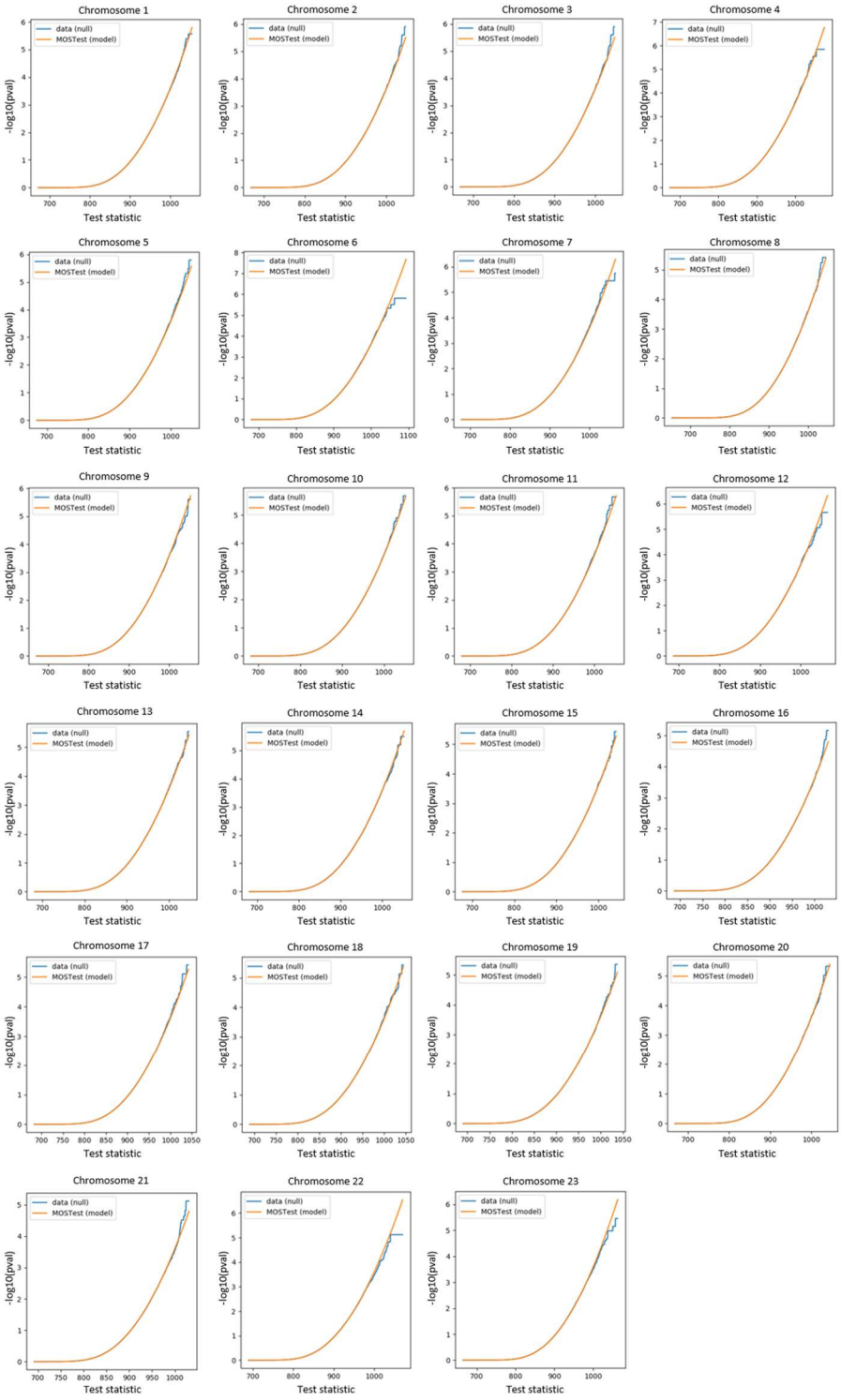


**Supplementary Figure 7. Permuted and analytic P value distributions under the null, for the multivariate GWAS of edge-level connectivity.** Only null distributions are shown here, i.e. not the true association results. Close matching of the null p-value distributions from the permuted data (blue) and analytic forms (orange) indicate correct control of type 1 error. The analytic distribution can then be extrapolated to assess the significance of multivariate associations with far lower p values (see Methods). 'Chromosome 23' refers to chromosome X.

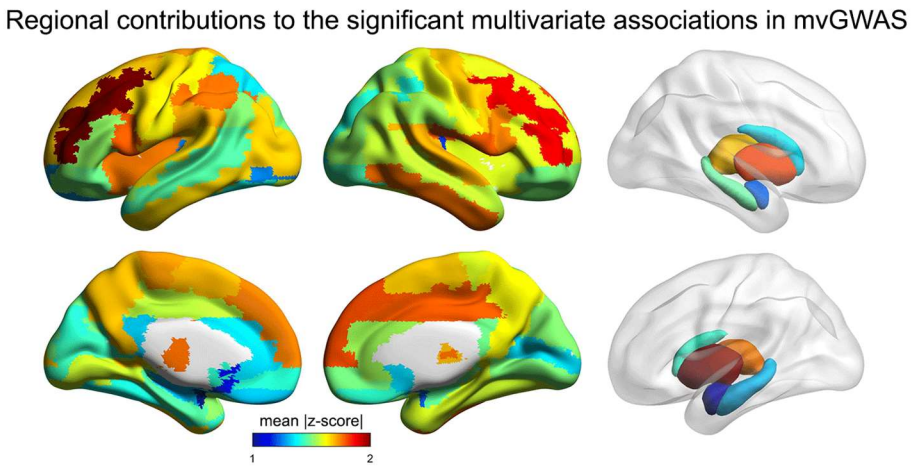


**Supplementary Figure 8. Regional contributions to the significant multivariate associations in the node-level connectivity mvGWAS**. For each region we calculated its average multivariate association z-score across all independently associated lead SNPs in the genome. This gives an indication of which node-level connectivities tend to be more often associated with genomic loci in general.

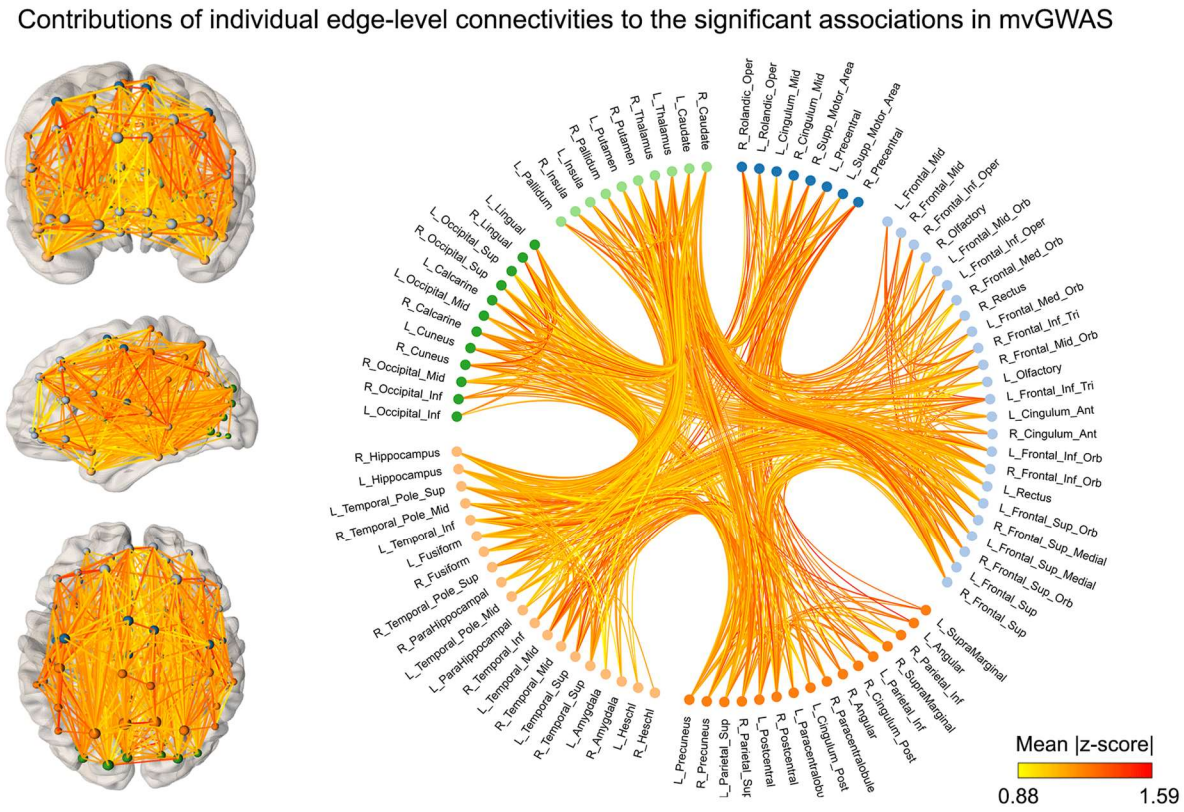


**Supplementary Figure 9. Contributions of individual edge-level connectivities to the significant multivariate associations in mvGWAS.** For each edge we calculated its average multivariate association z-score across all independently associated lead SNPs in the genome. This gives an indication of which edges tend to be more often associated with genomic loci in general. Left panel: brain maps. Right panel: nodes grouped by different anatomical lobes (frontal, prefrontal, parietal, temporal, occipital cortices, and subcortical structures).

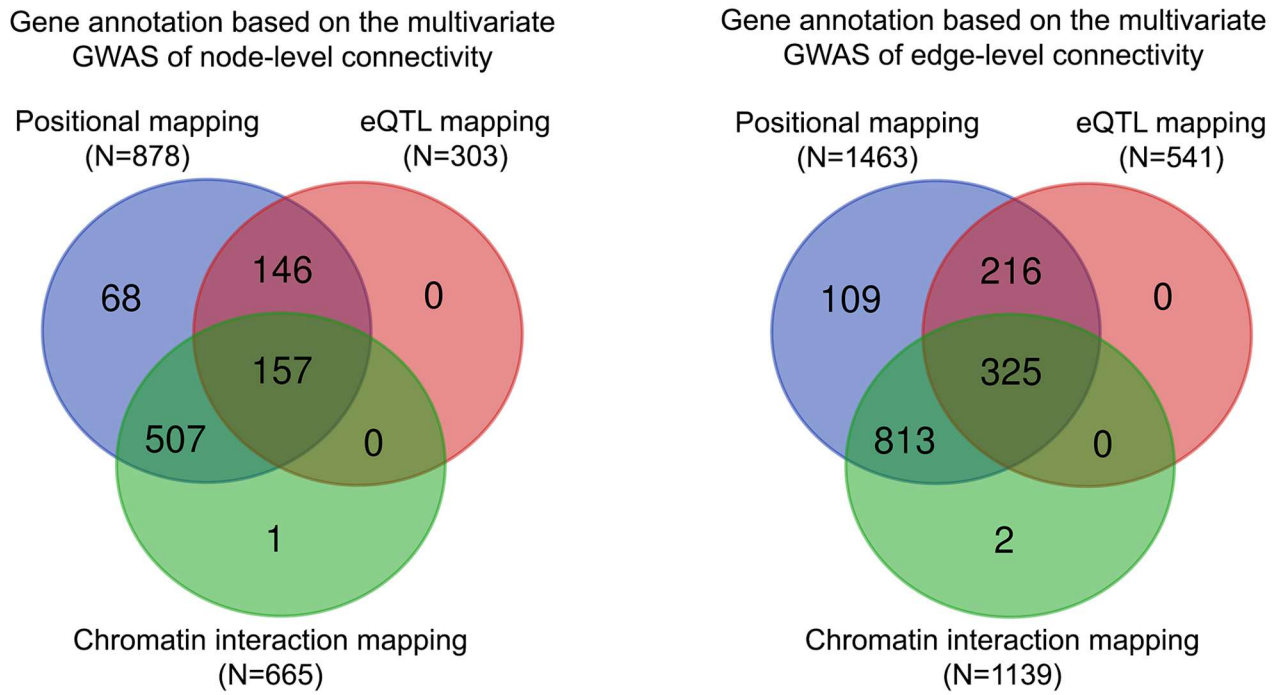


**Supplementary Figure 10. Numbers of annotated genes at significantly associated genomic loci using three mapping strategies in FUMA.** Left panel: annotated genes for significantly associated genomic loci in the multivariate GWAS of node-level connectivity. Right panel: annotated genes for significantly associated genomic loci in the multivariate GWAS of edge-level connectivity.

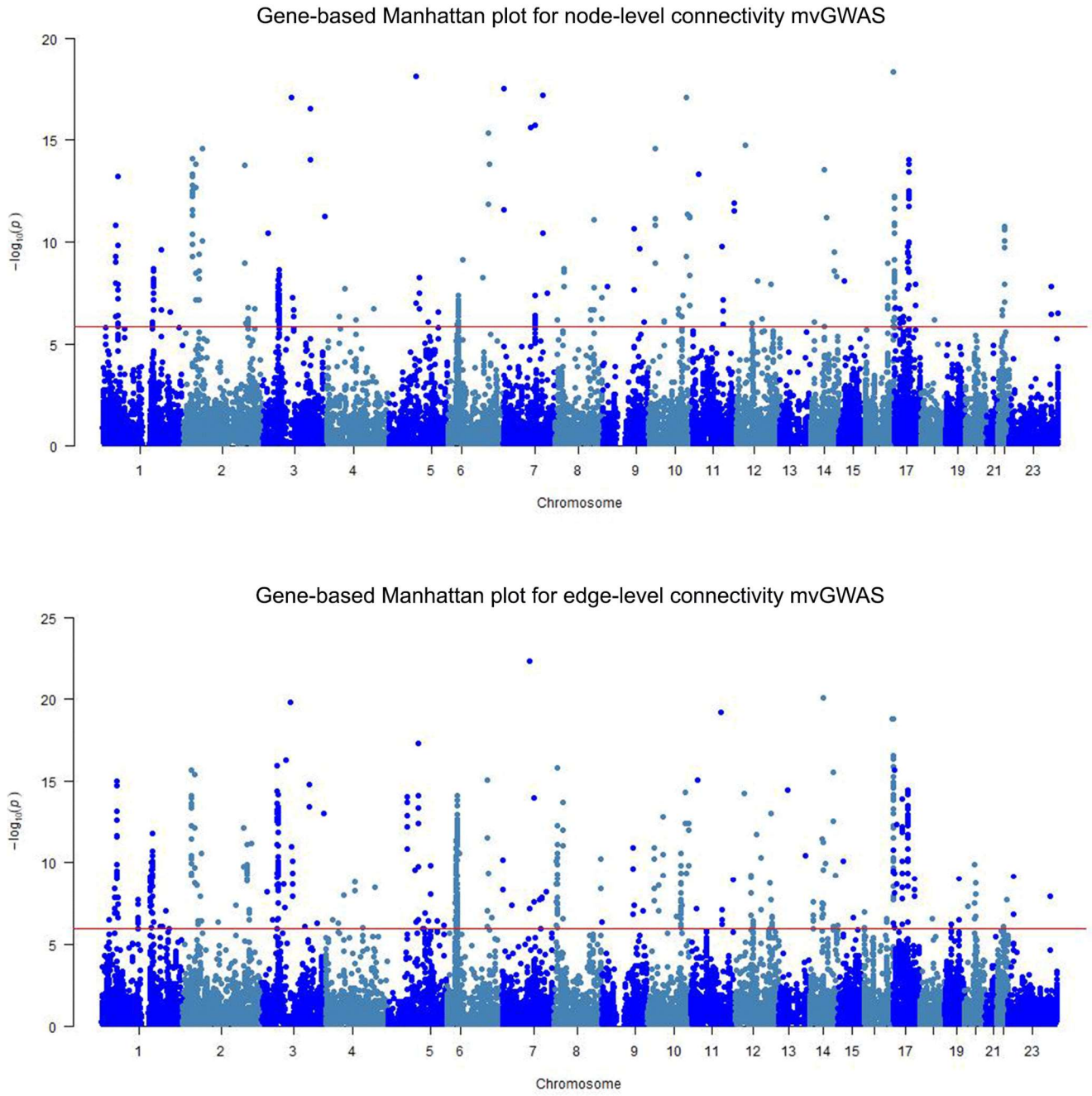


**Supplementary Figure 11. Manhattan plots for genome-wide gene-based association analysis, separately using the node-level connectivity mvGWAS (upper) and edge-level connectivity mvGWAS (lower) results as input.** The red line indicates the Bonferroni-corrected significance threshold for gene-based analysis of 20,146 genes ($p<0.025/20,146$).

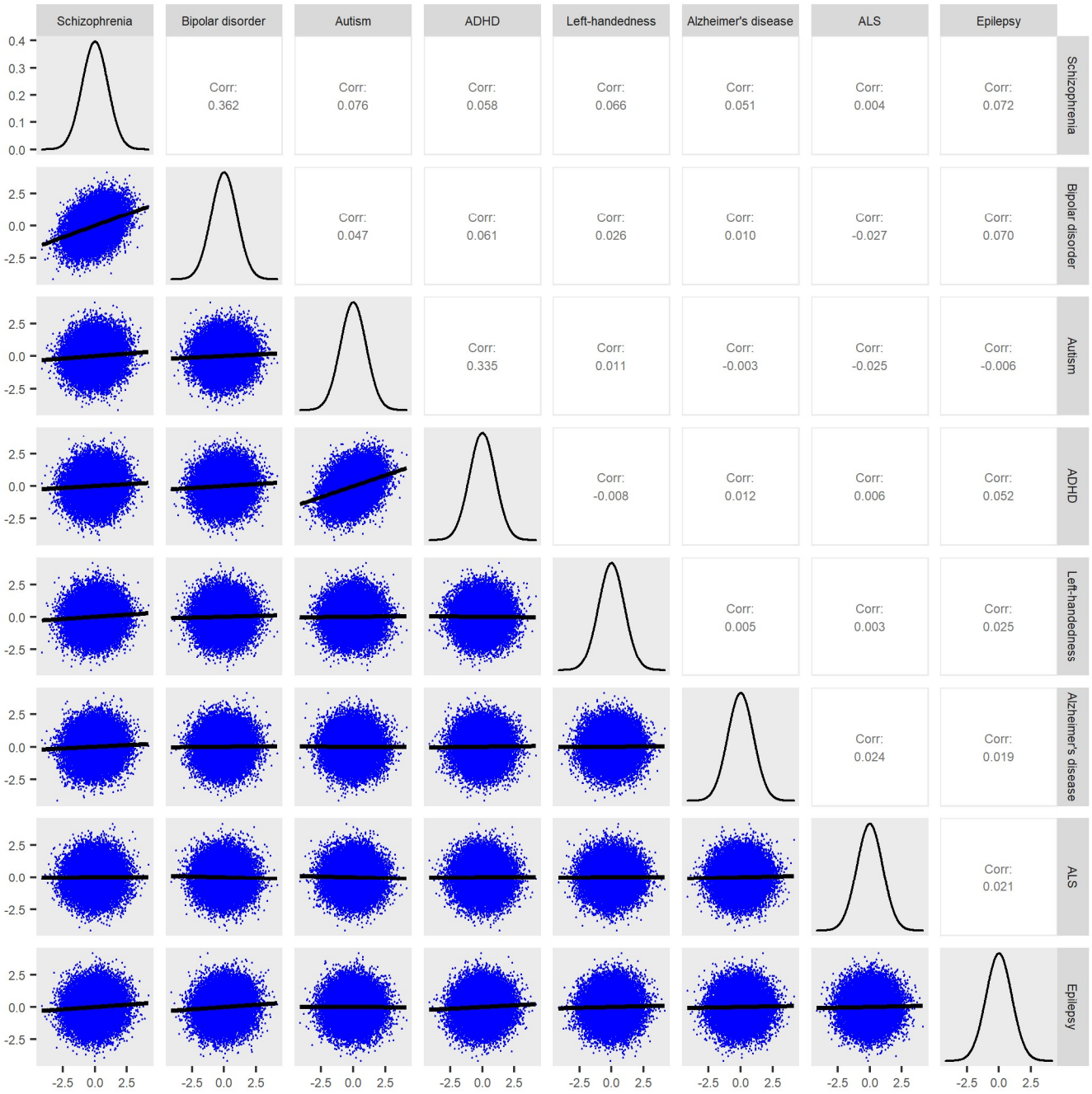


**Supplementary Figure 12. Partial correlations between normalized polygenic scores for brain-related disorders or behavioral traits.** Confounds including sex and age have been removed – see Methods. The diagonal of the matrix shows the distributions of the polygenic scores across the 30,810 individuals.

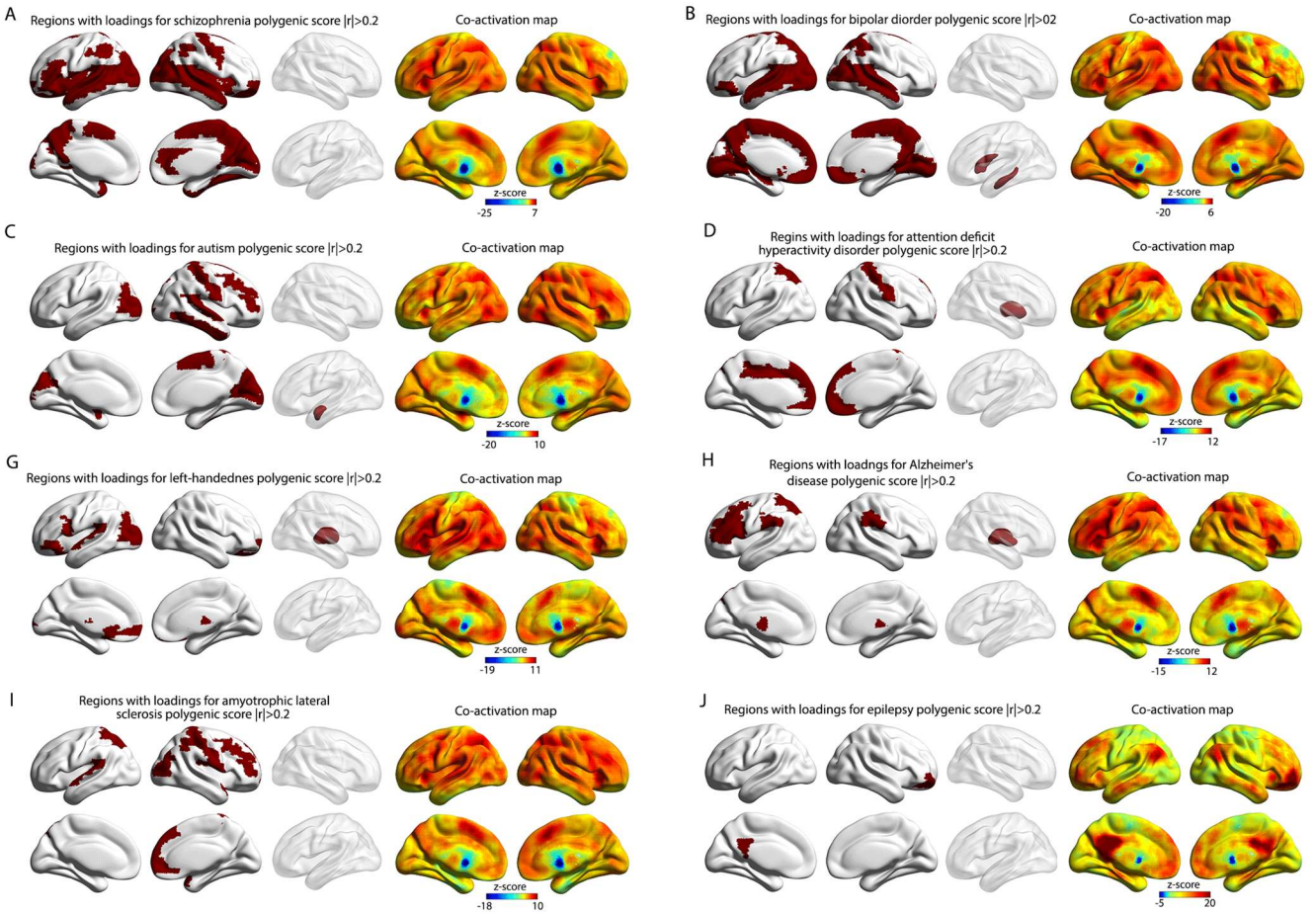


**Supplementary Figure 13. Node-level connectivities showing the strongest associations with polygenic scores for brain-related disorders or behavioral traits.** Left panel: Regions with loadings |r|>0.2 in canonical correlation analysis of their connectivities with a given polygenic score. The regional maps were used to define binary masks to query the Neurosynth database of meta-analyzed functional neuroimaging data from thousands of published studies. Right panel: Brain co-activation maps derived from the "decoder" function of Neurosynth, corresponding to the input masks.

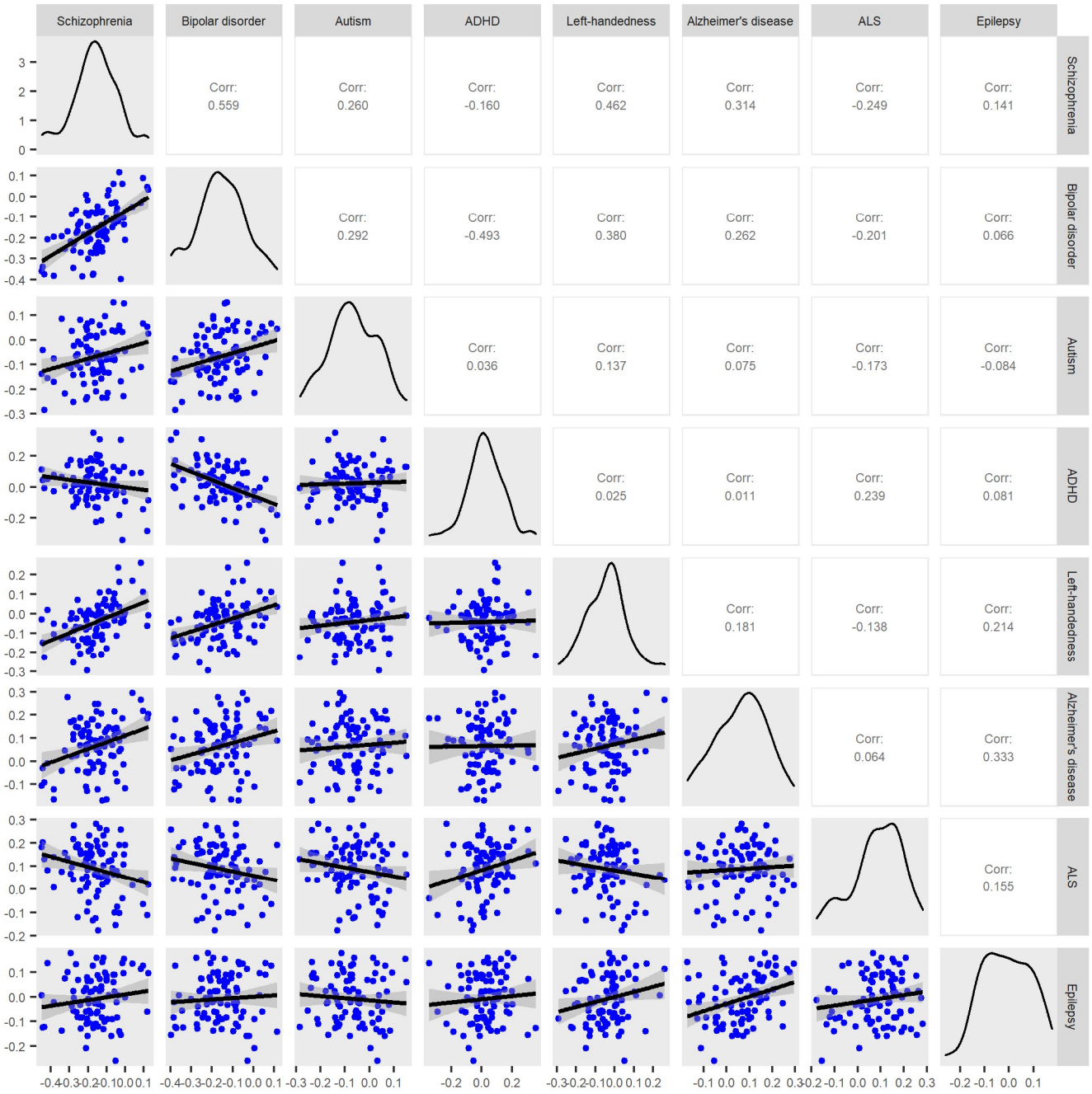


**Supplementary Figure 14. Correlations between the loadings derived from different canonical correlation analyses between polygenic scores and node-level connectivities.** These correlations are calculated over 90 brain regions. They show the extents to which polygenic dispositions to two different disorders/behaviors tend to associate consistently with the same brain regions. The diagonal of the matrix shows the distributions of loadings across regions.

**Supplementary Tables 1-31. All supplementary tables are given in one separate Excel file. Their contents are as follows:**

**Supplementary Table 1.** Node-level connectivity of the structural connectome.
**Supplementary Table 2.** SNP-based heritability estimates for node-level connectivity.
**Supplementary Table 3.** SNP-based heritability estimates for edge-level connectivity.
**Supplementary Table 4.** Significance of SNP-based heritability estimates for edge-level connectivities.
**Supplementary Table 5.** Standard errors of SNP-based heritability estimates for edge-level heritabilities.
**Supplementary Table 6.** 95% confidence interals of SNP-based heritability estimates for edge-level heritabilities.
**Supplementary Table 7.** Intraclass correlation coefficients from reliability analysis for node-level connectivity.
**Supplementary Table 8.** Intraclass correlation coefficients from reliability analysis for edge-level connectivity.
**Supplementary Table 9.** Lead SNPs from multivariate GWAS of node-level connectivity.
**Supplementary Table 10.** Lead SNPs from multivariate GWAS of edge-level connectivity.
**Supplementary Table 11.** Univariate association z scores for each lead SNP and node-level connectivities.
**Supplementary Table 12.** Univariate association z scores for each lead SNP and edge-level connectivities.
**Supplementary Table 13.** Regional contributions to the significant multivariate associations from node-level connectivity mvGWAS.
**Supplementary Table 14.** The contributions of individual edges to the significant multivariate associations from edge-level connectivity mvGWAS.
**Supplementary Table 15.** Lead SNPs associated with either node-level connectivity or edge-level connectivity in the present study that were also associated with white matter microstructure in reference *10* (see main text).
**Supplementary Table 16.** Gene mapping at all significant node-level connectivity mvGWAS loci based on three strategies.
**Supplementary Table 17.** Gene mapping at all significant edge-level connectivity mvGWAS loci based on three strategies.
**Supplementary Table 18.** Significant genes from gene-based analysis of node-level connectivity mvGWAS results.
**Supplementary Table 19.** Results from MAGMA gene set analysis, using node-level connectivity multivariate GWAS as input.
**Supplementary Table 20.** Significant genes from gene-based analysis of edge-level connectivity multivariate GWAS results.
**Supplementary Table 21.** Results from MAGMA gene set analysis, using edge-level connectivity multivariate GWAS as input.
**Supplementary Table 22.** Differential expression of genes associated with node-level connectivity in different lifespan stages from BrainSpan brain samples.
**Supplementary Table 23.** Differential expression of genes associated with edge-level connectivity in different lifespan stages from BrainSpan brain samples.
**Supplementary Table 24.** Differential expression of genes associated with node-level connectivity in different cell types in the developing human brain.
**Supplementary Table 25.** Differential expression of genes associated with edge-level connectivity in different cell types in the developing human brain.
**Supplementary Table 26.** Lead SNPs showing significant association with at least one core language network tract connectivity, and genes annotated to these lead SNPs by genomic position, eQTL and chromatin interaction.
**Supplementary Table 27.** Correlations between polygenic scores for brain-related disorder or behavioural traits.
**Supplementary Table 28.** Loadings from the canonical correlation analyses between node-level connectivities and polygenic dispositions to brain-related disorders or behavioural traits.
**Supplementary Table 29.** Loadings from the canonical correlation analyses between node-level connectivities and polygenic dispositions for Alzheimer's disease after excluding the APOE locus.
**Supplementary Table 30.** Functional terms based on meta-analyzed fMRI data, associated with co-activation maps for brain regions where node-level connectivity had loadings $|r|>0.2$ for polygenic scores of brain-related disorders or behavioural traits.
**Supplementary Table 31.** Correlation coefficients (across 90 regions) between loadings from multivariate associations of node-level connectivities with polygenic dispositions to brain-related disorders or behavioural traits.